Photoreactivity of Cyanoacetylene Trapped in Water Ice: An Infrared, Isotopic and Theoretical Study

Zohra Guennoun,* Nathalie Piétri, Isabelle Couturier-Tamburelli, and Jean-Pierre Aycard

UMR CNRS 6633, Physique des Interactions Ioniques et Moléculaires, Equipe de Spectrométries et Dynamique Moléculaires, Université de Provence, Case 252, Centre de St-Jérôme, 13397 Marseille Cedex 20, France

Received: May 31, 2005; In Final Form: July 11, 2005

Photoreactivity of cyanoacetylene with water was successively studied in cryogenic matrixes and in the solid phase at $\lambda > 120$ nm. These studies were performed using FTIR spectroscopy, isotopic experiments and DFT calculations at the B3LYP/6-31G** level of theory. The photolysis of cyanoacetylene complexed with water in an argon cryogenic matrix led to the formation of two products. The first one corresponds to the cyanoketene and the second to the HCN:C_2O complex. Trapped in water ice and submitted to UV photolysis, the cyanoacetylene molecule shows great photoreactivity. Indeed, besides the cyanoketene and cyanhydric acid, we characterized and identified the formation of other compounds issued from the addition of water to the C≡C triple bond of cyanoacetylene.

1. Introduction

Astronomical observations have shown the presence of numerous organic molecules in the interstellar medium, particularly in the dense and cold (10−90 K) molecular clouds.[1] Active chemistry takes place on grain mantles,[2] essentially constituted of water, and can be enriched by energetic processing such as cosmic rays. Among the interstellar molecules, cyanopolyynes and their chemistry are found in a variety of astrochemical environments and have been used to understand many observations made in diverse areas of astronomy and planetary sciences.[3] Within the solar system, nitrile chemistry is particularly relevant to Titan. Indeed, this saturnian satellite has a dense atmosphere,[4] essentially composed of N_2 (≅90%) and CH_4 (≅2%), which allows nitrile formation because it is subject to cosmic and solar radiations, UV photons and the saturnian magnetosphere. The arrival of the Cassini−Huygens orbiter and probe in January 2005 has also increased interest in Titan atmosphere simulations because this mission will provide numerous additional data on both gaseous and solid phases.[5]

Four gas-phase nitriles have already been identified in Titan's atmosphere: HCN, CH_3CN, HC_3N and C_2N_2, and a fifth, C_4N_2, has been detected as a solid.[6] These essential constituents in building block amino acids are particularly helpful for understanding Titan's chemistry. In addition, H_2O has recently been detected in this satellite.[7] Water ice can play a role in the photochemistry of species trapped in its lattice. Indeed, water acting as a reactive cage, the photofragments can react with nearest H_2O molecules.[8] Furthermore, photolyzed with UV radiation below 200 nm,[9] water ice dissociates and water photoproducts can react with the photofragments of the trapped molecules.

According to previous works, upon UV irradiation, cyanoacetylene (HC_3N), a key prebiotic synthesis molecule,[10] induces the formation of radicals $H^\bullet$ and $C_3N^\bullet$ at $\lambda > 120$ nm.[11] Therefore, the cyanoacetylene molecule complexed with water in cryogenic matrixes or trapped in water ice could induce photoreactivity and compounds such as cyanoketene and cyanhydric acid are expected to be formed. Thus, to investigate the formation of these two compounds at these wavelengths, we focus on the photoreactivity of cyanoacetylene trapped in water ice.

2. Experimental Section

Pure cyanoacetylene (CA) was synthesized using the methods described by Moureu and Bongrand[12] and was distilled before each deposition.

H_2O was doubly distilled before use. D_2O (99.8%) was supplied by SDS and used without further purification. Water and D_2O were degassed by successive freeze−thaw cycles under vacuum before each use.

Experimental Techniques. The apparatus and experimental techniques used to obtain argon matrixes have been described elsewhere in the literature.[13] The gas mixtures were prepared using standard manometric techniques. We obtained relative concentrations of CA/$H_2O(D_2O)$/Ar (1/20/650) and CA/$H_2O(D_2O)$ (1/5) sprayed by codeposition onto a golden copper plate cooled to 20 K. A Fourier transform infrared spectrometer (Nicolet series II Magna system 750) was used to record the spectra samples cooled to 10 K by reflectance in the range 4000−650 cm^{-1} with a resolution of 0.12 cm^{-1} for the argon matrixes and with a resolution of 1 cm^{-1} for the H_2O (D_2O) matrixes.

Irradiation Technique. UV irradiations of the matrixes were carried out using a microwave discharge hydrogen flow lamp (Opthos Instrument), adapted directly onto the sample chamber, which simulates the interstellar irradiation field. The flux of this lamp transmitted through the MgF_2 window ($\lambda > 120$ nm) is considered in the range from 3 to 10 eV, and its spectrum is dominated by two bands centered around 120 and 160 nm.[14]

3. Results and Discussion

The matrix isolation spectroscopy technique has been shown to constitute a very successful approach for studying photo-

* To whom any correspondence should be addressed. E-mail: zohra.guennoun@up.univ-mrs.fr. Phone number: (+33) 4.91.28.85.83. Fax number: (+33) 4.91.63.65.10.

10.1021/jp0528820 CCC: $30.25
Published on Web 08/30/2005

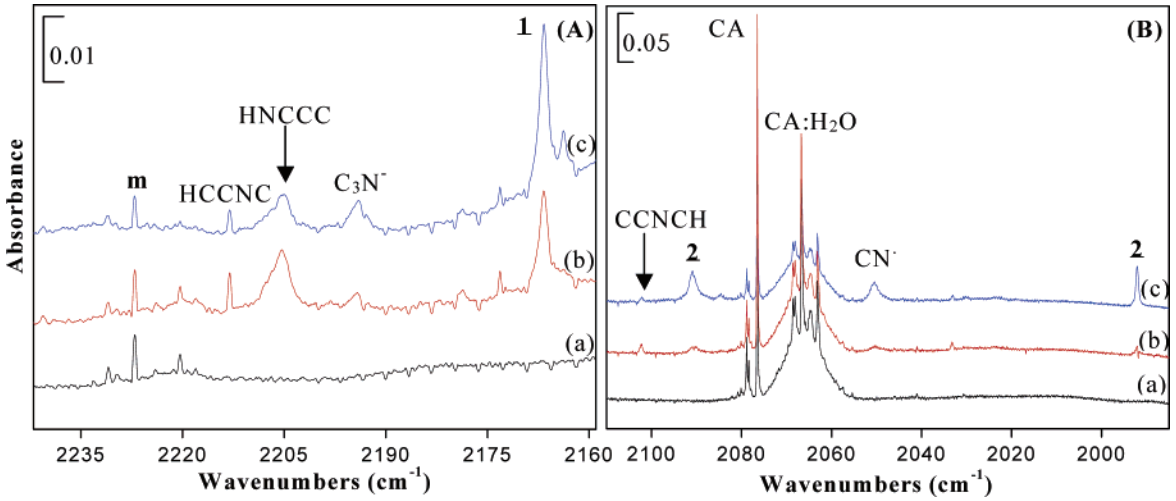

Figure 1. Infrared spectra in different areas of the CA:H_2O complexes photolysis products isolated in argon matrix at 10 K before and after photolysis at $\lambda > 120$ nm: (a) CA/H_2O/Ar (1/20/650) reference spectrum; (b) CA/H_2O/Ar (1/20/650) after 81 min of irradiation; (c) CA/H_2O/Ar (1/20/650) after 1013 min of irradiation. The band denoted by "**m**" is assigned to the multimers of cyanoacetylene.

chemical processes, taking advantage of the very low working temperature, which allows the trapping of reactive and unstable compounds. Furthermore, this technique has advantages both for identification and characterization of photochemical reactions, such as photodegradation and rearrangement reactions, and for the study of photochemically induced conformational isomerization processes. Thus, to make it easier to analyze the results of the photolysis of cyanoacetylene trapped in water ice, we first carry out the UV irradiations on cyanoacetylene:H_2O complexes in cryogenic matrixes.

Matrixes containing only CA, H_2O or D_2O were prepared, yielding infrared absorption spectra that were similar to those previously reported for the monomers[15,16] and for the CA:H_2O (D_2O) complexes, characterized in argon matrix by Borget et al.[15]

The electronic absorption spectrum of CA comprises two intense absorption bands centered at 145 nm (very strong) and 161 nm (medium)[17] and two other weak features[18] at 226 and 260 nm. Although we studied the photoreactivity of CA with water at different wavelengths, we present here the most interesting results obtained at $\lambda > 120$ nm.

3.1. Photoreactivity of CA with Water in Argon Matrix. *3.1.1. Experimental Results.* During the photolysis of a CA/H_2O/Ar mixture, we observe the decrease of the CA, H_2O and CA:H_2O complexes' absorption bands.[19] Issued from UV irradiations of CA and H_2O monomers, respectively, we note the formation of isomers of CA (HCCNC,[20] HNCCC[21] and CCNCH[22]) and species such as OH•, HOO•, OH^- [23] and H_2O_2[24] (Figure 1). In addition, during the experiment we note the growing of new bands situated at 2167, 2090 and 1992 cm^{-1}, which probably come from the complexes' photolysis (Figure 1).

The band located at 2167 cm^{-1} could be attributed to the ν(CCO) stretching mode of cyanoketene (**1**) (Figure 1A, Scheme 1A) according to our previous results obtained by irradiation of dicyanoacetylene:H_2O complexes[25] and the literature.[26] The weak absorbance of this band, which is the most intense of cyanoketene, does not allow us to observe the other, much weaker, bands of this compound.

The two other bands, 2090 and 1992 cm^{-1} (Figure 1B), which present the same kinetic behavior during irradiation, could respectively be assigned to the cyanhydric acid and the C_2O species. Indeed, the HCN molecule, trapped in an argon matrix, is characterized in the infrared region by an absorption band at

SCHEME 1: Mechanisms of Formation of the Cyanoketene and the C_2O:HCN Complex by Photolysis of the CA:H_2O Complexes at $\lambda > 120$ nm in an Argon Matrix

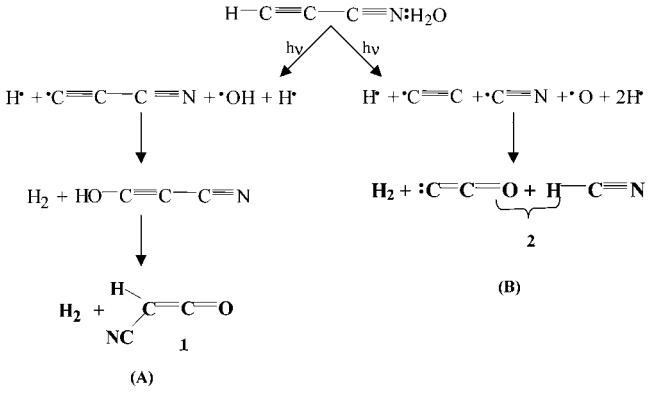

2098 cm^{-1} (ν(C≡N)),[27] and the C_2O species by an intense band at 1978 cm^{-1} (ν(CCO)).[28] These two compounds are probably obtained by the respective additions of the H• and O• radicals, coming from the photodissociation of H_2O, to the •CN and C_2 species, produced by photolysis of CA (Scheme 1B). Furthermore, it is interesting to note that the ν(C≡N) stretching mode of HCN is shifted by 8 cm^{-1} toward lower frequencies and the ν(CCO) mode of C_2O by 14 cm^{-1} toward higher frequencies with respect to the data of the literature. Therefore, we can assume that these frequency shifts are due to the formation of a HCN:C_2O complex (**2**).

To confirm our results, we perform the photolysis of the CA:D_2O complexes in an argon matrix. During this experiment, we observe the increase of a band at 2160 cm^{-1}, which confirms the D-cyanoketene formation according to the literature[25,26] (Scheme 1A).

Finally, we detect two other bands with the same behavior at 1992 and 1892 cm^{-1}. The first one, observed in the photolysis of the CA:H_2O complexes, was not modified by the presence of D_2O whereas the absorption band of HCN (2090 cm^{-1}) disappeared, moving to 1892 cm^{-1}, which proves the DCN formation. Moreover, this last band is shifted by 30 cm^{-1} toward lower frequencies with respect to the DCN absorption band observed in argon matrix[29] at 1922 cm^{-1}. Thus, all these results allow us to conclude on the probable DCN:C_2O complex formation during photolysis of the CA:D_2O complexes (Scheme 1B).

CHART 1: Optimized Geometries of HCN Complexed with C_2O Obtained for the CH and OH Structures at the B3LYP/6-31G Level of Theory[a]**

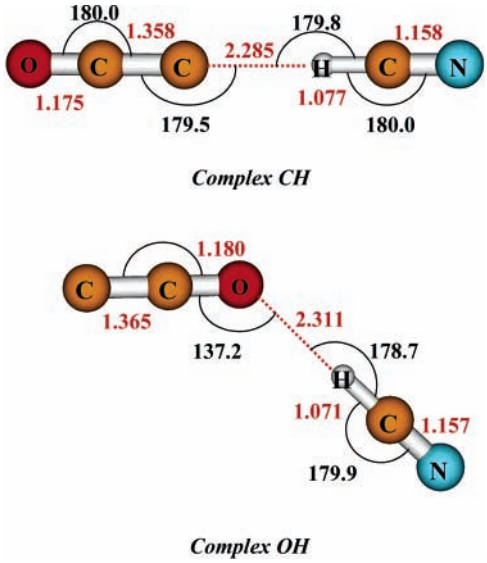

[a] The lengths and angles are given in Å and degrees, respectively.

3.1.2. Identification of the HCN:C_2O Complex by DFT Calculations. Our experimental results in the argon matrix indicate the formation of a HCN:C_2O complex. To model its structure and its vibrational spectrum, theoretical calculations were carried out (B3LYP/6-31G**) on different starting geometries for each complex. For an AB complex, the stabilization energy is calculated as follows: $\Delta E = E(AB) - E^{BSSE}(A) - E^{BSSE}(B)$, where $E^{BSSE}(A)$ and $E^{BSSE}(B)$ are the energies of the A and B moieties corrected of the basis set superposition error (BSSE).[30] For each minimum energy structure, normal coordinate calculations were carried out. The resulting vibrational frequencies remained unscaled.

Calculations yield only two local minima. The optimized structures are shown in Chart 1. The first one, corresponding to the linear shape (CH complex), exhibits a hydrogen bond between the carbon atom of C_2O and the hydrogen atom of HCN, which is calculated to be 2.285 Å. The second one, called OH complex, is characterized by a hydrogen bond involving the oxygen atom of C_2O and the hydrogen atom of HCN. This bond was calculated to be 2.311 Å. In these two structures, the C_2O molecule acts as a proton acceptor and the HCN acts as a proton donor. At last, the CH complex is predicted to be more stable than the OH one by 11.6 kJ·mol^{-1}.

The calculated harmonic frequencies of the monomers and those of the C_2O:HCN (C_2O:DCN) complexes are summarized in Table 1. It is worthwhile to note the good agreement between the experimental and calculated frequency shifts for the CH complex. Indeed, the theoretical frequencies of the OH complex are slightly modified with respect to those calculated for the monomers contrary to the CH complex for which the ν(CN) and ν(CCO) stretching modes of HCN and C_2O, respectively, are shifted by -10 and $+18$ cm^{-1} (Table 1). These are in better agreement with the experimental results: -8 and $+14$ cm^{-1}. Moreover, the frequency shifts calculated for the CD complex are similar to those observed in our experiment for the DCN:C_2O complex (Table 1).

3.2. Photoreactivity of CA with Water in H_2O Matrix. *3.2.1. Experimental Results.* During the photolysis of CA/H_2O at $\lambda > 120$ nm, we observe the decrease of the CA and H_2O absorption bands and the growth of numerous bands. Indeed, we note the formation of two bands situated at 2166 and 2088 cm^{-1} that grow until the end of photolysis (Figure 2A). These were respectively attributed to the cyanoketene **1** and HCN **3** by analogy with the previous results. During the experiment, we also observe the growing of absorption bands at 2222, 1659, 1626, 1333, 1252, 1206 and 1111 cm^{-1} which behave as a reaction intermediate (Figure 2). Among these bands, those situated at 2222 and 1659/1626 cm^{-1} are respectively characteristic of C≡N and C═C stretching modes whereas the other ones are probably due to stretching C—O modes (1333/1255 cm^{-1}) and C—C modes (1204/1111 cm^{-1}). Thus, we hypothesize that these bands could be due to the formation of enols, obtained by the addition of a H_2O molecule to the triple CC bond of CA. Therefore, two compounds could be formed: 2-hydroxyacrylonitrile (**4**) and 3-hydroxyacrylonitrile (**5**) (Scheme 2).

At last, we observe the increase of a band at 1730 cm^{-1}, which grows until the end of the irradiation. Characteristic of a C═O stretching mode of a carbonyl compound, this could be issued from the keto—enolic equilibrium. Indeed, a tautomeric rearrangement of the 2-hydroxyacrylonitrile and the 3-hydroxyacrylonitrile leads respectively to the formation of pyruvonitrile (**6**) and cyanoacetaldehyde (**7**) (Scheme 2).

It is interesting to note that we do not observe the formation of the isomers of CA.[20−22] This result could be explained by the fact that the radicals (H$^\bullet$ and $C_3N^\bullet$), produced by the cleavage of the H—C bond of CA, react with water as soon as they are formed, making the observation of these isomers impossible.

Annealing of the sample enhances the absorption bands of the enolic and ketonic compounds. After sublimation of CA and water ices near 200 K, only the bands of the cyanoketene (**1**) and ketonic and enolic products remain in the IR spectrum (Figure 3), which allow us to observe the presence of other bands at 3052 and 967 cm^{-1} that could be attributed to the enolic compounds (Table 2).

We performed the isotopic experiment irradiating the CA trapped in D_2O matrix to confirm our experimental results and to identify the photoreactivity products (Figure 4). This experiment leads to the formation of the D-cyanoketene[26] observed at 2158 cm^{-1}. We also note during photolysis the growth of bands situated at 1637 and 1614 cm^{-1}, which present the same kinetic behavior (Table 3). These are probably due to the enolic compounds. As previously observed, by annealing the sample the absorbance of the IR bands of the enolic compounds increase. After sublimation of the CA and D_2O ices, we observe the presence of bands at 2221, 1328, 1268, 1228 and 1152 cm^{-1} probably due to the enolic compounds (Figure 3, Table 3). At last, we observe the growing of a band at 1730 cm^{-1} that is not shifted with respect to that one obtained in the CA/H_2O photolysis (Figure 3). These bands, growing during the annealing, were not observed by irradiation because of the presence of D_2O absorption bands in the 2760−2270 and 1600−1160 cm^{-1} areas.

3.2.2. Identification of the Photoreactivity Products. 3.2.2.1. Identification of the Enolic Compounds. Previous works[31,32] showed that the triple CC bond of cyanoacetylene is especially susceptible to nucleophilic attack by an hydroxide ion. Thus, the cyanoacetylene in dilute aqueous base is hydrolyzed to the 3-hydroxyacrylonitrile (**5**), which leads to the cyanoacetaldehyde (**6**) (Scheme 2). No infrared data of these compounds have been reported in the literature. Thus, to characterize by infrared spectroscopy these molecules, we performed calculations (B3LYP/6-31G**) and performed an experiment on CA in dilute aqueous solution at room temper-

TABLE 1: Experimental (exp) and Calculated (cal) Frequency Shifts (cm^{-1}) for the CH (CD) and OH (OD) C_2O:HCN Complexes at the B3LYP/6-31G Level of Theory[a]**

	experimental				theoretical (B3LYP/6-31G(d,p))							
		complex			monomers		complexes				$\Delta\nu_{cal}$	
	monomers[27,28] ν	ν	(I)[b]	$\Delta\nu_{exp}$	ν	(I)[b]	CH	(I)[b]	OH	(I)[b]	CH	OH
HCN	3306				3476	(100)	3354	(100)	3448	(100)	−122	−28
	2098	2090	36	−8	2212	(4)	2202	(9)	2212	(7)	−10	0
	721				769	(64)	926	(5)	820	(17)	−157	−51
C_2O	1978	1992	100	14	2042	(100)	2060	(21)	2042	(53)	18	0
	1074				1117	(39)	1149	(6)	1116	(24)	32	−1

	experimental				theoretical (B3LYP/6-31G(d,p))							
		complex			monomers		complexes				$\Delta\nu_{cal}$	
	monomers[27,28] ν	ν	(I)[b]	$\Delta\nu_{exp}$	ν	(I)[b]	CD	(I)[b]	OD	(I)[b]	CD	OD
DCN	2631				2755	(100)	2695	(100)	2741	(72)	−60	−14
	1923	1892	17	−31	2011	(39)	1975	(75)	2005	(51)	−36	−6
	572				613	(50)	731	(6)	647	(11)	118	34
C_2O	1978	1992	100	14	2042	(100)	2060	(65)	2042	(100)	18	0
	1074				1117	(39)	1149	(19)	1116	(49)	32	−1

[a] $\Delta\nu = \nu$(complex) − ν(monomer). [b] Experimental and theoretical integrated intensities are in % from the strongest band.

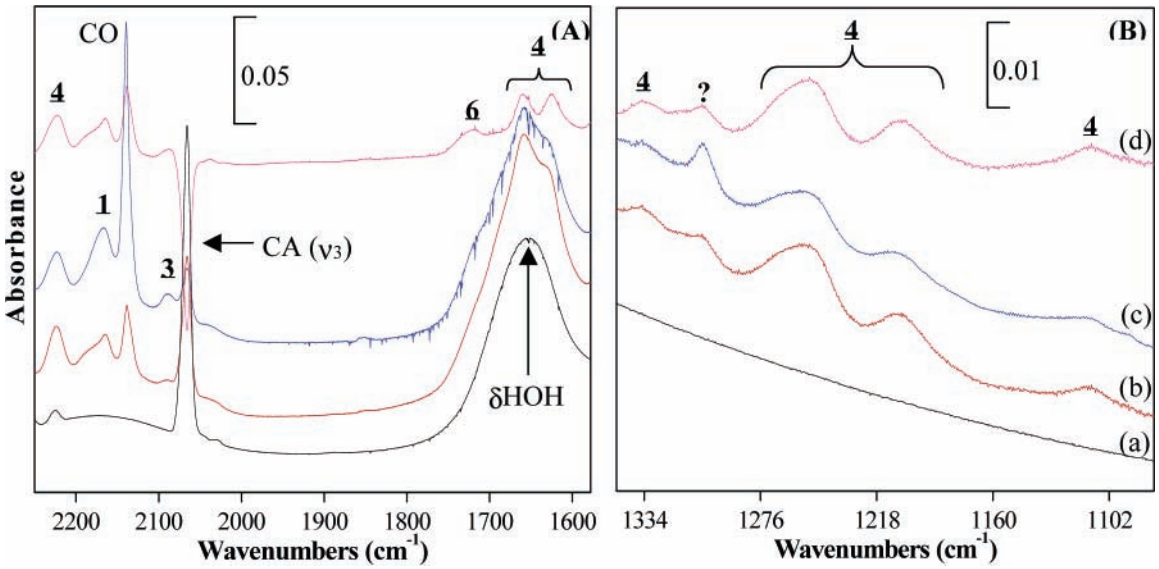

Figure 2. Infrared spectra obtained by irradiation of a CA/H_2O mixture at 10 K before and after irradiation at $\lambda > 120$ nm: (a) CA/H_2O (1/5) reference spectrum; (b) CA/H_2O (1/5) after 260 min of irradiation; (c) CA/H_2O (1/5) after 1050 min of irradiation; (d) subtraction (c) − (a).

SCHEME 2: Mechanisms of Formation of the Possible Enolic and Keto−Nitrile Compounds Issued from Irradiation of a CA/H_2O Mixture at $\lambda > 120$ nm

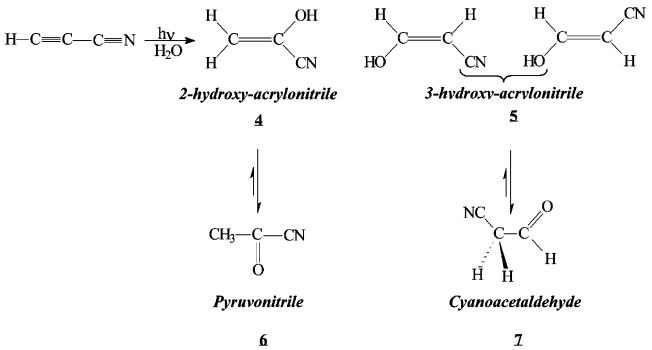

ature. This experiment led to the formation of an enol identified as the *cis*-3-hydroxyacrylonitrile by NMR spectroscopy. Two conformers of this enolic compound (A and B) were optimized (Chart 2). Contrary to the conformer B, the molecule A displays the hydrogen atom of the alcohol function in interaction with the cyano group. In addition, calculations predict the conformer A to be more stable than the conformer B by 17.4 kJ·mol^{-1}. At last, the analysis of the data reported in Table 4 shows a good agreement between the experimental frequencies of the enol formed in solution with those calculated for the conformer A.

On the other hand, the comparison between the IR spectrum obtained in solution and that in the photolysis experiment allows us to conclude that the enol formed in our experiment is not the 3-hydroxyacrylonitrile. So, we investigated the formation of the 2-hydroxyacrylonitrile (**4**) by performing calculations that led to the optimization of two conformers: C and D (Chart 3).

Each conformer is characterized by calculated frequencies clearly distinct from the other form (Table 2). In agreement with these calculated values, it can be established that the enol produced during photolysis is trapped in water ice as a mixture of these two conformers. Indeed, we observe two bands in the ν(C═C) area: 1659 and 1626 cm^{-1}, which could be attributed to the C and D conformers, respectively. The most interesting range to determine the presence of the two conformers is the

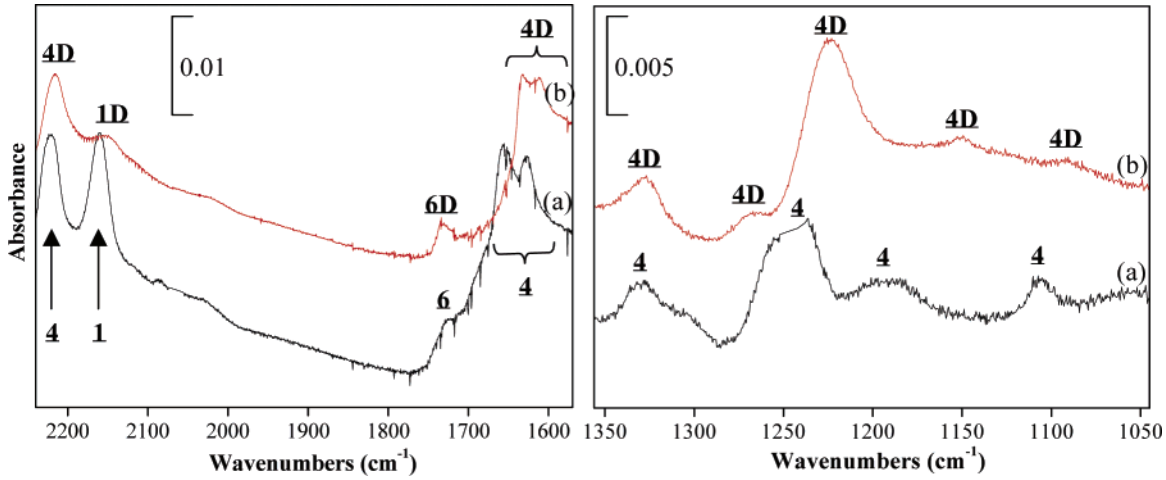

Figure 3. Infrared spectra obtained by annealing at 200 K after photolysis of a CA/H_2O mixture (a) and after photolysis of a CA/D_2O mixture (b).

TABLE 2: Comparison between Experimental Frequencies (cm^{-1}) of the 2-Hydroxyacrylonitrile and the Frequencies of Its Conformers C and D Calculated at the B3LYP/6-31G Level of Theory**

	scaled ν	
exp ν obtained during photolysis of CA/H_2O[b]	conformer C[a,b]	conformer D[a,b]
	3681 (35)	3659 (22)
	3169 (<1)	3154 (<1)
3052 (15)	3070 (1)	3053 (2)
2222 (41)	2250 (5)	2269 (2)
1659 (100)	1657 (19)	
1626 (27)		1635 (56)
	1381 (2)	1393 (5)
1333 (9)		1350 (11)
1255 (15)	1288 (100)	
1204 (8)	1188 (12)	
1111 (4)		1141 (100)
967 (12)	945 (17)	948 (10)

[a] Experimental and theoretical integrated intensities given between brackets are in % from the strongest band. [b] The frequencies are scaled with a factor of 0.96.

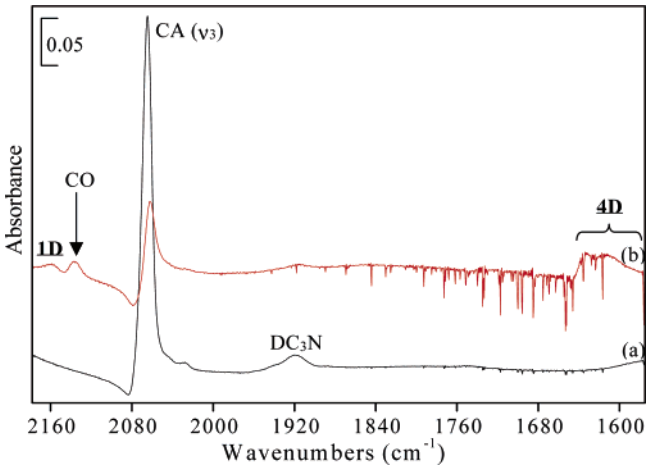

Figure 4. Infrared spectra obtained by irradiation of a CA/D_2O mixture at 10 K before and after irradiation at $\lambda > 120$ nm: (a) CA/D_2O (1/5) reference spectrum; (b) CA/D_2O (1/5) after 1370 min of irradiation.

1350−1110 cm^{-1} one. Indeed, the bands observed at 1333 and 1111 cm^{-1} are characteristic of the C conformer and those obtained at 1255 and 1204 cm^{-1} confirm the presence of the D conformer. Unfortunately, the experimental intensities do not correlate with the theoretical ones because the calculations were carried out for the free molecule and, thus, they do not take account of the effect of the water cage in which the molecule is formed. Indeed, the geometry of the D conformer can be modified by the water cage, which can induce changes of its absorption bands intensities.

TABLE 3: Comparison between Experimental Frequencies (cm^{-1}) of the Deuterated 2-Hydroxyacrylonitrile and the Frequencies of Its Conformers Calculated at the B3LYP/6-31G Level of Theory[a]**

	scaled ν			
exp ν obtained during photolysis of CA/D_2O[a]	conformer C-cis[a,b]	conformer C-trans[a,b]	conformer D-cis[a,b]	conformer D-trans[a,b]
	3129 (1)	3083 (5)	3132 (1)	3112 (1)
	2663 (28)	2663 (28)	2681 (58)	2681 (61)
	2271 (8)	2305 (4)	2292 (3)	2308 (3)
2221 (63)	2269 (3)	2270 (5)	2250 (14)	2250 (15)
1637 (100)	1633 (99)	1636 (100)		
1614 (54)			1616 (66)	1617 (71)
1328 (13)	1353 (76)	1368 (40)	1371 (81)	1379 (100)
1268/1228 (65)	1256 (19)	1291 (67)	1273 (100)	1278 (84)
1152 (2)	1093 (100)	1147 (85)	1147 (13)	1156 (56)
	892 (11)	907 (4)	904 (69)	918 (23)

[a] Experimental and theoretical integrated intensities given between brackets are in % from the strongest band. [b] The frequencies are scaled with a factor of 0.96.

TABLE 4: Comparison between Experimental Frequencies (cm^{-1}) of the *cis*-3-Hydroxyacrylonitrile and the Frequencies of Its Conformers Calculated at the B3LYP/6-31G Level of Theory[a]**

	scaled frequencies	
exp ν obtained in solution[a]	conformer A[a,b]	conformer B[a,b]
	3579 (17)	3696 (66)
	3112 (1)	3095 (2)
3067 (94)	3094 (1)	3051 (6)
2235 (65)	2233 (18)	2249 (16)
1600 (100)	1620 (100)	1669 (68)
1342 (34)	1373 (4)	1391 (3)
1331 (9)	1332 (<1)	1259 (100)
1192 (15)	1194 (70)	1210 (35)
	1074 (3)	1085 (19)
964 (45)	968 (37)	921 (6)
937 (5)	931 (3)	909 (≪1)

[a] Experimental and theoretical integrated intensities given between brackets are in % from the strongest band. [b] The frequencies are scaled with a factor of 0.96.

CHART 2: Optimized Geometries of Conformers A and B of *cis*-3-Hydroxyacrylonitrile at the B3LYP/6-31G Level of Theory[a]**

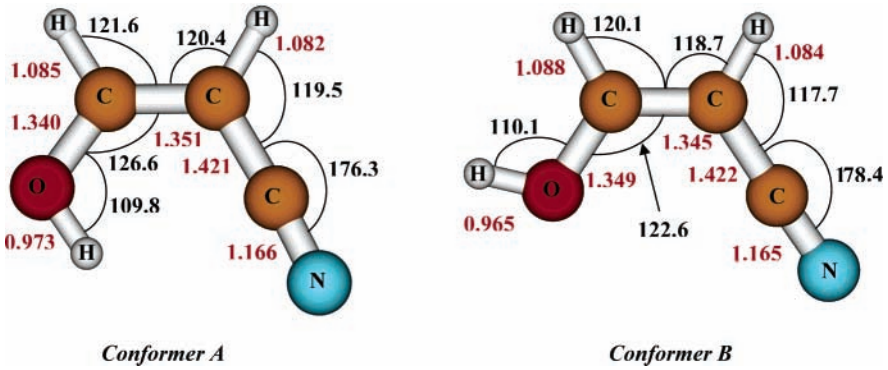

[a] The lengths and angles are given in Å and degrees, respectively.

CHART 3: Optimized Geometries of Conformers C and D of 2-Hydroxyacrylonitrile at the B3LYP/6-31G Level of Theory[a]**

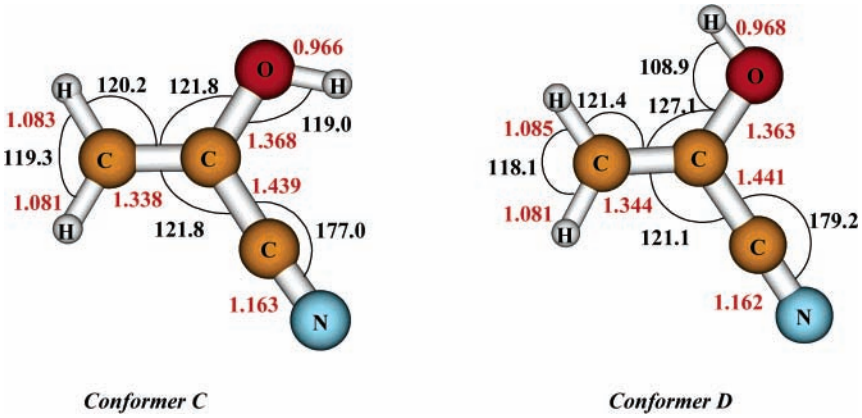

[a] The lengths and angles are given in Å and degrees, respectively.

CHART 4: Conformers *Z* and *E* for the Deuterated Enols C and D

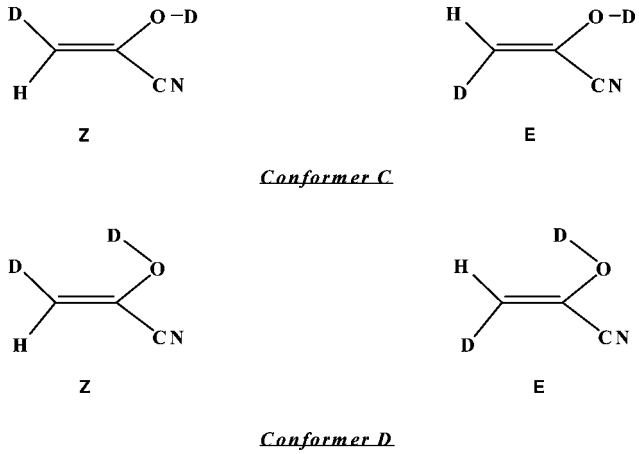

However, the irradiation of the CA trapped in D_2O led to the growing of absorption bands at 1637 and 1614 cm^{-1} for whom the frequency shifts, 22 and 12 cm^{-1}, with respect with that observed in H_2O matrix, are in good agreement with those calculated for the enols C and D respectively for their *Z* and *E* conformers (Chart 4), 24−21 and 19−18 cm^{-1} (Table 5). So, we conclude that the irradiation of CA in water ice leads to the formation of the 2-hydroxyacrylonitrile in the form of two isomers. Finally, the formation and the presence of these two conformers in our photolysis experiment can be explained by the little difference of stabilization energy between C and D. Indeed, conformer C is more stable than D by only 0.6 kJ·mol^{-1}.

TABLE 5: Experimental (exp) and Calculated (cal) Frequency Shifts (cm^{-1}) for the ν(C═C) Stretching Mode between Conformers C and D of 2-Hydroxyacrylonitrile

experimental			theoretical		
CA/H_2O	CA/D_2O	$\Delta\nu$	CA/H_2O	CA/D_2O	$\Delta\nu$
conformer C	conformer C		conformer C	conformer C (*Z*/*E*)	
1659	1637	22	1657	1633/1636	24/21
conformer D	conformer D		conformer D	conformer D (*Z*/*E*)	
1626	1614	12	1635	1616/1617	19/18

3.2.2.2. Identification of the Carbonyl Compound. According to the reactional mechanism proposed in Scheme 2, a tautomeric rearrangement of 2-hydroxyacrylonitrile (**4**) would lead to pyruvonitrile (**6**). Therefore, to confirm its formation we deposited at 10 K the pyruvonitrile (Aldrich 95%) trapped in a H_2O matrix (1/10). We noted that the infrared spectrum of this compound in water ice is dominated by an intense absorption band situated at 1729 cm^{-1}. It is worth noting the good agreement between this frequency and the one obtained during our experiment at 1730 cm^{-1}.

Furthermore, calculations of the vibrational frequencies of cyanoacetaldehyde (**7**) showed that the ν(C═O) stretching mode of this keto-nitrile is shifted by 44 cm^{-1} to higher frequencies, with respect to the C═O stretching mode of pyruvonitrile, and thus it is expected around 1775 cm^{-1} (Table 6). The non-observation of the growth of a band in this area and the unobserved shift of this band in the CA/D_2O photolysis, as

TABLE 6: Experimental and Calculated Frequencies (cm^{-1}) for the Cyanoacetaldehyde and the Pyruvonitrile in B3LYP/6-31G Basis Set[a]**

pyruvonitrile		cyanoacetaldehyde	
cal frequencies[a]	scaled frequencies[b]	cal frequencies[a]	scaled frequencies[b]
3174 (2)	3047	3075 (<1)	2952
3116 (1)	2991	3040 (5)	2918
3051 (<1)	2929	2927 (82)	2810
2343 (16)	2249	2385 (3)	2290
1809 (100)	1736	1853 (100)	1779
1470 (10)	1411	1446 (12)	1389
1401 (24)	1345	1331 (25)	1278
1202 (85)	1154	1004 (8)	964
987 (15)	947	837 (10)	804
720 (16)	691	734 (20)	705

[a] Experimental and theoretical integrated intensities given between brackets are in % from the strongest band. [b] The frequencies are scaled with a factor of 0.96.

predicted by calculations, reinforce the attribution of the band observed at 1730 cm^{-1} to the pyruvonitrile.

4. Discussion and Conclusion

Irradiations of CA complexed with water in argon matrix or trapped in water ice induce photochemical processes. Previous experiments showed that irradiations of CA induced photodissociation as reported in following equations:

$$HC_3N \rightarrow H^\bullet + {}^\bullet C_3N \quad (1)$$

$$HC_3N \rightarrow HC_2^\bullet + {}^\bullet CN \quad (2)$$

At $\lambda > 120$ nm, the breaking of the CH single bond of CA is the major process under UV photolysis[11] (eq 1). By the cleavage of the CC single bond, $^\bullet C_2H$ and $^\bullet CN$ radicals are obtained[11] (eq 2). Upon UV irradiation the H_2O molecule can also undergo photodissociation. Indeed, according to previous works,[9,33] the breaking of one single bond is the major process leading to the formation of $H^\bullet$ and $^\bullet OH$ species at these wavelengths. Nevertheless, a secondary photolysis process could produce $O^\bullet$ radicals.

The cyanoketene, observed by the CA:H_2O complexes irradiation in an argon matrix, is issued from tautomerization of the cyanoethynol, which is obtained by addition of the $^\bullet OH$ radical to the $^\bullet C_3N$ species (Scheme 1A). At last, by another photochemical reaction, we observed the formation of the C_2O:HCN complex. This product was obtained by addition of the $H^\bullet$ and $O^\bullet$ radicals to $^\bullet CN$ and C_2 species respectively (Scheme 1B).

In addition, the results obtained by photolysis in H_2O matrixes indicate that cyanoacetylene has more important photoreactivity when it is trapped in water ice than in argon matrixes. Besides the cyanoketene and HCN formation during this photolysis experiment, other compounds were formed and identified (Scheme 2). Indeed, UV irradiation performed at $\lambda > 120$ nm leads to the fragmentation of the H_2O molecule in $H^\bullet$ and $^\bullet OH$ radicals. These react with the C≡C bond of CA leading to the formation of two conformers of 2-hydroxyacrylonitrile and its tautomer: pyruvonitrile.

Lastly, it is interesting to note that the enolic compound formed in the photolysis experiments is different from that obtained in aqueous solution identified by Ferris et al.[31]

Acknowledgment. The theoretical part of this work was conducted with the technical means of "Centre régional de Compétence en Modélisation Moléculaire de Marseille".

References and Notes

(1) Ehrenfreund, P.; Huntress, W. T. *Space Sci. Rev.* **1999**, *90*, 209.

(2) Ehrenfreund, P.; Charnley, S. B. *Annu. Rev. Astron. Astrophys.* **2000**, *38*, 427.

(3) (a) Coll, P.; Coscia, D.; Smith, N.; Gazeau, M. C.; de Vanssay, E.; Guillemin, J. C.; Raulin, F. *Adv. Space Res.* **1995**, *16* (2) 93. (b) Yung, Y. L.; Allen, M.; Pinto, J. P. *Astrophys. J. Supp.* **1984**, *55*, 465. (c) Toublanc, D.; Parisot, J. P.; Brillet, J.; Gautier, D.; Raulin, F.; McKay, C. P. *Icarus* **1995**, *113*, 2. (d) Masterson, C. M.; Khanna, R. K. *Icarus* **1990**, *83*, 83.

(4) Samuelson, R. E. *Planet. Space Sci.* **2003**, *51*, 127.

(5) Bernard, J. M.; Coll, P.; Coustenis, A.; Raulin, F. *Planet Space Sci.* **2003**, *51*, 1003.

(6) Coustenis, A.; Schmitt, B.; Khanna, R. K.; Trotta, F. *Planet Space Sci.* **1999**, *47*, 1305.

(7) Coustenis, A.; Salama, A.; Lellouch, E.; Encrenaz, Th.; Bjoraker, G. L.; Samuelson, R. E.; de Graauw, Th.; Feuchtgruber, H.; Kessler, M. F. *Astron. Astrophys.* **1998**, *336*, L85.

(8) Schriver, A.; Coanga, J. M.; Schriver-Mazzuoli, L.; Ehrenfreund, P. *Chem. Phys. Lett.* **2004**, *386*, 377.

(9) (a) Andresen, P.; Schinke, R. *Molecular Photodissociation Dynamics* **1987**, *3*. (b) Mordaunt, D. H.; Ashfold, M. N. R.; Dixon, R. N. *J. Chem. Phys.* **1994**, *100*, 7360. (c) Hwang, D. W.; Yang, X. F.; Harich, S.; Lin, J. J.; Yang, X. *J. Chem. Phys.* **1999**, *110*, 123. (d) Harich, S. A.; Hwang, D. W. H.; Yang, X.; Jin, J. J.; Yang, X.; Dixon, R. N. *J. Chem. Phys.* **2000**, *113*, 10073.

(10) Orgel, L. E. *Origins Life* **2002**, *32*, 279.

(11) (a) Halpern, J. B.; G. E. Miller, H. Okabe, J. Photochem. Photobio. A. **1988**, *42*, 63. (b) Halpern, J. B.; Petway, L.; Lu, R.; Jackson, W. M.; McCrary, V. R. *J. Phys. Chem.* **1990**, *94*, 1869.

(12) Moureu, C.; Bongrand, J. C. *Ann. Chim.* Paris **1920**, *14*, 47.

(13) Piétri, N.; Jurca, B.; Monnier, M.; Hillebrand, M.; Aycard, J. P. *Spectrochim. Acta* **2000**, *A56*, 157.

(14) (a) Hagen, W.; Allamandola, L. J.; Greenberg, J. M. *Astrophys. Space Sci.* **1979**, *65*, 215. (b) Jenniskens, P.; Baratta, G. A.; Kouchi, A.; De Groot, M. S.; Greenberg, J. M.; Strazulla, G. *Astron. Astrophys.* **1993**, *273*, 583.

(15) (a) Borget, F. Thesis, Université de Provence, 2000. (b) Borget, F.; Chiavassa, T.; Aycard, J.-P. *Chem. Phys. Lett.* **2001**, *348*, 425.

(16) (a) Devlin, J. P.; Buch, V. *J. Phys. Chem.* **1997**, *101*, 16534. (b) Devlin, J. P.; Buch, V. *J. Phys. Chem.* **1995**, *99*, 6095.

(17) Connors, R. E.; Rebber, J. L.; Weiss, K. J.*Chem. Phys.* **1974**, *60*, 5011.

(18) (a) Job, V. A.; King, G. W. *J. Mol. Spectrosc.* **1966**, *19*, 155. (b) Job, V. A.; King, G. W. *J. Mol. Spectrosc.* **1966**, *19*, 178.

(19) Borget, F.; Chiavassa, T.; Allouche, A.; Marinelli, F.; Aycard, J. P. *J. Am. Chem. Soc.* **1996**, *118*, 10668.

(20) Kolos, R.; Waluk, J. *J. Mol. Struct.* **1997**, *408/409*, 473.

(21) Kolos, R.; Sobolewski, A. L. *Chem. Phys. Lett.* **2001**, *344*, 625.

(22) Guennoun, Z.; Couturier-Tamburelli, I.; Piétri, N.; Aycard, J. P. *Chem. Phys. Lett.* **2003**, *36*, 574.

(23) Suzer, S.; Andrews, L. *J. Chem. Phys.* **1988**, *88*, 916.

(24) Smith, D. W.; Andrews, L. *J. Chem. Phys.* **1974**, *60*, 81.

(25) Guennoun, Z.; Piétri, N.; Couturier-Tamburelli, I.; Aycard, J. P. *Chem. Phys.* **2004**, *300*, 23.

(26) Maier, G.; Reisenauer, H. P.; Rademacher, K. *Chem. Eur. J.* **1998**, *10*, 1957.

(27) Satoshi, K.; Takayanagi, M.; Nakata, M. *J. Mol. Struct.* **1997**, *365*, 413.

(28) Jacox, M. E.; Milligan, D. E.; Moll, N. G.; Thomson, W. E. *J. Chem. Phys.* **1965**, *43*, 3734.

(29) King, C. M.; Nixon, E. R. *J. Chem. Phys.* **1968**, *48*, 1685.

(30) Boys, S.; Bernardi, F. *Mol. Phys.* **1970**, *19*, 553.

(31) (a) Ferris, J. P.; Sanchez, R. A.; Orgel, L. E. *J. Mol. Biol.* **1968**, *33*, 693. (b) Ferris, J. P.; Zamek, O. S.; Altbuch, A. M.; Freiman, H. *J. Mol. Evol.* **1974**, *3*, 301.

(32) Guillemin, J. C.; Bouyahyi, M.; Riague, E. H. *Adv. Space Res.* **2004**, *33*, 81.

(33) (a) Harich, S. A.; Hwang, D. W. H.; Yang, X.; Jin, J. J.; Yang, X.; Dixon, R. N. *J. Chem. Phys.* **2000**, *113*, 10073. (b) Krautwald, H. J.; Schnieder, L.; Welge, K. H.; Ashfold, M. N. R. *Faraday Discuss. Chem. Soc.* **1986**, *82*, 99.